ELSEVIER

Computer Communications 25 (2002) 1037–1046

computer communications

www.elsevier.com/locate/comcom

Bandwidth allocation in a multiservice satellite network based on long-term weather forecast scenarios

Raffaele Bolla[a], Nedo Celandroni[b], Franco Davoli[a,*], Erina Ferro[b], Mario Marchese[c]

[a]*Department of Communications, Computer and Systems Science (DIST), University of Genoa, Via Opera Pia 13, 16145 Genoa, Italy*
[b]*CNUCE Institute of National Research Council (CNR), CNR Research Area, Via Moruzzi 1, 56010 Pisa, Italy*
[c]*CNIT—Italian National Consortium for Telecommunications, University of Genoa Research Unit, Via Opera Pia 13, 16145 Genoa, Italy*

Received 1 August 2001; revised 30 October 2001; accepted 28 November 2001

Abstract

The paper compares two alternative hierarchical bandwidth allocation and admission control schemes suited for the multiservice Ka-band satellite environment, where the attenuation of the transmitted signals due to bad weather conditions has a heavy impact on the system's performance. The two schemes are compared by using data derived from a real case study. The aim is to demonstrate that a high level control mechanism for the assignment of the satellite bandwidth to earth stations, which takes into consideration the rain attenuation probabilities of a certain geographical area, improves the system's performance, with respect to an assignment mechanism insensitive to the geographical fade probabilities.

Keywords: Satellite communications; Bandwidth control; Fade; Rain probability; Performance thresholds

1. Introduction

Broadband satellite networks are becoming an important segment of the global telecommunication infrastructure, due to their wide geographical coverage and configuration flexibility. They provide seamless integration of applications and services that have traditionally been available via terrestrial networks. With respect to the latter, satellite networks present two main problems: the round trip delay (250–280 ms for geostationary satellites), which heavily affects the real-time transmissions, and the effects of the bad weather conditions in transmissions in the Ka frequency band. In the Ka band, fade countermeasure techniques must be developed for guaranteeing an acceptable quality of service (QoS) of the transmitted data even in faded conditions [1,2].

In this work, we consider a very small aperture terminal (VSAT) satellite network, where the traffic stations do not actually communicate with each other directly, but via a more powerful hub station, towards which data transmissions from the traffic stations are concentrated and then redistributed. Two types of traffic are considered: a QoS guaranteed traffic, modeled as synchronous transmission operating at a fixed speed, and a non-guaranteed best-effort traffic, modeled by an aggregated flow with self-similar characteristics [3]. Each traffic station conveys the traffic flows coming both from traffic sources (i.e. PCs, workstations, video cameras), directly connected to the station, and from LANs.

Fade due to bad weather conditions may be a very quick event that may degrade the system in few seconds. In this work, we assume that stations do not continuously check their fade level, in order to send the hub requests for a bandwidth assignment able to dynamically follow the fade's shape. The only information about their status transmitted by the traffic stations to the hub is a binary one (clear sky or rain). In one of the two schemes analyzed, the fade problem is faced at a higher level: on a large time scale, the hub station assigns satellite bandwidth to the traffic stations according to the statistic probability of fade associated to their geographical position, besides considering the traffic loads. In the other scheme, the geographical positions of the stations, along with the fade probabilities associated to them, are not taken into account, and the bandwidth is assigned on the basis of the traffic load only. In both schemes, each traffic station distributes the portion of the bandwidth assigned by the hub between its real-time and non-real-time traffic. Both the hub assignment and the local bandwidth distribution must keep the call blocking

* Corresponding author. Tel.: +39-103-532-732; fax: +39-103-532-154.
E-mail addresses: nedo.celandroni@cnuce.cnr.it (N. Celandroni), franco@dist.unige.it (F. Davoli), erina.ferro@cnuce.cnr.it (E. Ferro), mario.marchese@cnit.it (M. Marchese), lelus@dist.unige.it (R. Bolla).

0140-3664/02/$ - see front matter
PII: S0140-3664(02)00018-X

probability of the guaranteed traffic below a given threshold and must minimize the packet discarding probability of the best effort portion. They attempt to do so by solving a constrained numerical optimization problem, with a suitable cost function. From the performance management and control point of view, this scheme falls in the category of dynamic hierarchical bandwidth assignment and call admission in multiservice networks [4–9], (see also [6–9], among others, for similar, non-hierarchical, control approaches). However, to the best of the authors' knowledge, no such scheme has been proposed so far as dynamic fade countermeasure in the satellite environment.

The fading is modeled by assigning a probability of channel degradation to the in-bound link only, along with a weighting coefficient to 'measure' the degradation itself. In the numerical results presented, we consider real data from traffic stations of the Lario type (northern Italy), which have a relatively higher rain probability. For these stations, the probabilities to be in a certain range of fade values are obtained from measurements on a 5-year basis, performed in the framework of the Sirio satellite experimentation program. The effectiveness of the a-priori information on the fade level is evaluated by averaging over all possible scenarios, whose empirical probabilities are derived by long-term measurements.

The paper is organized as follows. We introduce our traffic models and related performance measures in Section 2. Sections 3 and 4 are dedicated to the description of the control schemes to be implemented in the hub and in the traffic stations, respectively. Section 5 contains the details of the real case study, whose data are used in the numerical calculations reported in Section 6. Section 7 is dedicated to the conclusions.

2. Real-time traffic, best-effort traffic, blocking and loss probabilities

Each synchronous connection is defined as continuous bit rate (CBR) flows at B (kbit/s), which must be reserved to each connection to guarantee the proper level of quality of service. The traffic of each station i, $i = 1, \ldots, N$ (where N is the number of stations that compete for bandwidth) is considered to be independent of the others. Let $\lambda^{(i)}$ (s^{-1}) be the arrival rate of the connection requests, $1/\mu^{(i)}$ (s) the average duration of each connection, and $\rho^{(i)} = \lambda^{(i)}/\mu^{(i)}$ the traffic intensity (Erlang), for station i. As customary to represent the dynamics at the connection level, exponential distributions are used both for the inter-arrival time and the service time, with the time variable assumed continuous. If $N^{(i)}_{\max}$ is the maximum number of calls acceptable at station i, the call blocking probability experienced by it is

$$P^{(i)}_B\left(N^{(i)}_{\max}\right) = \frac{(\rho^{(i)})^{N^{(i)}_{\max}}/N^{(i)}_{\max}!}{\sum_{n=0}^{N^{(i)}_{\max}} (\rho^{(i)})^n/n!} \tag{1}$$

As far as the asynchronous non-guaranteed traffic is concerned, we suppose that it originates from datagrams, which are fragmented into ATM cells before transmission on the satellite channel. At each station i, cells are queued in a buffer and, in this context, the quantity of interest is the cell loss probability of the non-guaranteed traffic in the queue of station i. In order to derive an approximate evaluation of this quantity, we consider a self-similar traffic model, which represents the superposition of an infinite number of on–off sources, with Pareto-distributed 'on' time and exponentially distributed 'off' time, respectively. The detailed description of the model can be found in Refs. [3,10]. Let us define a time interval $T = L/B_{\text{ng}}$, where L is the length of the non-guaranteed traffic transmission unit (bit), and B_{ng} the peak generation rate of each asynchronous source (bit/s). If $\lambda^{(i)}_{\text{burst}}$ is the rate (burst/s) of the asynchronous traffic at station i, the birth rate of the process $\lambda^{(i)}_{\text{ng}}$, i.e. the average number of sources which become active, entering an on period, during the interval T, is

$$\lambda^{(i)}_{\text{ng}} = \lambda^{(i)}_{\text{burst}} T \tag{2}$$

Let us define the variable

$$X^{(i)} = \frac{C^{(i)}_{\text{ng}}}{L} T = \frac{C^{(i)}_{\text{ng}}}{L} \frac{L}{B_{\text{ng}}} = \frac{C^{(i)}_{\text{ng}}}{B_{\text{ng}}}$$

$C^{(i)}_{\text{ng}}$ being the capacity variable for the asynchronous traffic of station i (bit/s), which we suppose to be an integer multiple of B_{ng}. If $\lambda^{(i)}_{\text{ng}}\tau^m < X^{(i)}$, where τ^m is the average duration of the on period, the overflow probability of the buffer dedicated to the asynchronous traffic, $P^{(i)}_{\text{over}}$, is bounded asymptotically in $Q^{(i)}$ by [10]:

$$P^{(i)}_{\text{over}} \le \frac{c\lambda^{(i)}_{\text{ng}}}{\alpha(\alpha-1)\left(X^{(i)} - \lambda^{(i)}_{\text{ng}}\tau^m\right)} (Q^{(i)})^{-\alpha+1} \tag{3}$$

where α is the parameter of the discrete-time Pareto distribution, c is its normalization constant, and Q is the length of the buffer itself. Formula (3) shows a bound in the case of a very large buffer and describes an asymptotic behavior.

We define now the following quantity, to be used in the cost functions adopted by the two control schemes in the following:

$$P^{(i)}_{\text{loss}}(X^{(i)}) = \begin{cases} \min\left\{ \dfrac{c\lambda^{(i)}_{\text{ng}}}{\alpha(\alpha-1)\left(X^{(i)} - \lambda^{(i)}_{\text{ng}}\tau^m\right)} (Q^{(i)})^{-\alpha+1}, 1 \right\} & \text{if } X^{(i)} > \lambda^{(i)}_{\text{ng}}\tau^m \\ 1 & \text{otherwise} \end{cases} \tag{4}$$

The bandwidth allocated to the non-guaranteed traffic at station i ($C^{(i)}_{\text{ng}}(t)$) at time t is actually a random variable, as it depends on the number $n^{(i)}(t)$ of guaranteed traffic connections in progress at station i at the same instant.

$$C^{(i)}_{\text{ng}}(t) = C^{(i)} - Bn^{(i)}(t) \tag{5}$$

where $C^{(i)}$ is the total capacity allocated to station i. Thus, also the quantity $X^{(i)}$ should be assumed time-variant. Time has been inserted to underline the fact that the non-guaranteed traffic always takes the residual bandwidth not used, at any given instant, by the guaranteed traffic. The time index will be dropped, where not explicitly necessary.

The process $n^{(i)}(t)$ can assume only discrete values from 0 to $N^{(i)}_{\max}$; as a consequence, $C^{(i)}_{\rm ng}(t)$ only assumes discrete values with a certain probability, depending on the probability of having $n^{(i)}(t)$ connections in progress at time t at station i. If we indicate by $X^{(i)}_j$, the realization of the variable $X^{(i)}(t)$, corresponding to $n^{(i)}(t) = j$, we have:

$$X^{(i)}_j = \frac{C^{(i)}}{B_{\rm ng}} - \frac{B}{B_{\rm ng}} j, \qquad j = 0, 1, \ldots, N^{(i)}_{\max} \tag{6}$$

and

$$\Pr\left\{X^{(i)}(t) = X^{(i)}_j\right\} = \Pr\{n^{(i)}(t) = j\} \tag{7}$$

where $\Pr\{n^{(i)}(t) = j\}$ is given by the stationary distribution of a $M/M/N^{(i)}_{\max}/N^{(i)}_{\max}$ queuing system.

We assume as an indication of the packet loss rate at station i the quantity defined in Eq. (4), averaged over the number of guaranteed connections:

$$\bar{P}^{(i)}_{\rm loss}\left(C^{(i)}_{\rm ng}, N^{(i)}_{\max}\right) = \sum_{j=0}^{N^{(i)}_{\max}} P^{(i)}_{\rm loss}\left(X^{(i)}_j\right)\Pr\{n^{(i)}(t) = j\} \tag{8}$$

The loss probability depends on the threshold $N^{(i)}_{\max}$ and on the overall bandwidth $C^{(i)}$ allocated to station i. Even the latter quantities may be (slowly) time-variant, should the bandwidth be reallocated on-line, on the basis of changes in the channel characteristics. However, the holding time of given values of $C^{(i)}$ (and, consequently, of $N^{(i)}_{\max}$) may well be considered infinite with respect to the dynamics of the process $n^{(i)}(t)$. Moreover, it is worth noting that, in writing Eq. (8), we have exploited the fact that the time scales of the guaranteed and non-guaranteed traffic are widely different, in order to use independent stationary distributions for both traffics. In other words, the guaranteed traffic process is supposed to be quasi-stationary in computing Eq. (4), and the non-guaranteed traffic queue is supposed to reach steady-state between successive jumps in the Markov chain of the former [4,11].

3. The control schemes implemented in the hub

An upper level control scheme is implemented in the hub station. It periodically allocates the available bandwidth C (bit/s) by assigning a portion $C^{(i)}$ (bit/s) of the total bandwidth to each earth station i. The algorithms considered for the allocations are the optimal channel-adaptive bandwidth allocation in satellite channels (OC-ABASC), simply indicated in the following as OC, and the constrained average probability-adaptive bandwidth allocation in satellite channels (CAP-ABASC) method, indicated as CAP [12]. The first method does not take into account any degradation of the satellite link, as, instead, the CAP method does. Both methods perform the allocations by minimizing a different cost function, described in Sections 3.1 and 3.2. In the CAP method, the fading effect on the channel 'seen' by station i is modeled as a reduction of the capacity $C^{(i)}$ allocated. The real capacity utilized by station i may be written as $C^{(i)}_{\rm real} = \beta^{(i)}_{\rm level} C^{(i)}$, where $\beta^{(i)}_{\rm level}$ is a coefficient, ranging over a number of possible values (indicated by the subscript 'level'), weighting the levels of channel degradation (e.g. the data redundancies due to the decreased bit coding rates); to each value $\beta^{(i)}_{\rm level}$, a probability $p^{(i)}_{\rm level}$ is associated. We remind here that in this analysis the fading is not intended as instantaneous, but it is described by the probability that a certain station has to be in a given range of fade values, owing to its geographical position.

Before discussing the cost functions minimized in the hub station, we give a few definitions useful in the following. If $Z^{(i)}$ is a generic variable, the function $N^{(i)}_{\max}(Z^{(i)})$ is defined as:

$$N^{(i)}_{\max}(Z^{(i)}) = \begin{cases} \left\lfloor C^{(i)}_{\min}/B \right\rfloor & \text{if } C^{(i)}_{\min} < Z^{(i)} \\ \lfloor Z^{(i)}/B \rfloor & \text{if } C^{(i)}_{\min} \geq Z^{(i)} \end{cases} \tag{9}$$

where $C^{(i)}_{\min}$ is the minimum bandwidth needed to obtain a call blocking probability lower than a given threshold $\gamma^{(i)}$, and $\lfloor x \rfloor$ is the largest integer less than or equal to x.

3.1. The cost function in the OC case

From Eqs. (8) and (9), indicating the dependence on $Z^{(i)}$, let

$$J^{(i)}(Z^{(i)}) = \begin{cases} \bar{P}^{(i)}_{\rm loss}\left[C^{(i)}_{\rm ng}(Z^{(i)}), N^{(i)}_{\max}(Z^{(i)})\right] & \text{if } Z^{(i)} \geq C^{(i)}_{\min} \\ H & \text{if } Z^{(i)} < C^{(i)}_{\min} \end{cases} \tag{10}$$

be the cost function for station i, where H is a large number (with respect to the other quantities involved; an order of magnitude of 10 may serve the purpose). The overall cost function is:

$$J_{\rm OC}(Z^{(1)}, Z^{(2)}, \ldots, Z^{(N)}) = \sum_{i=1}^{N} J^{(i)}(Z^{(i)}) \tag{11}$$

We assume $Z^{(i)} \in \mathscr{R} : Z^{(i)} = k$ mbp, $\forall k \in N$, $Z^{(i)} \leq C$, where 'mbp' is the minimum bandwidth portion that can be allocated, and represents the granularity of the algorithm. The aim is to find the particular values of $Z^{(i)} = C^{(i)}$ that minimize the function (11), under the constraints

$$\begin{cases} \sum_{i=1}^{N} Z^{(i)} = C \\ Z^{(i)} \geq 0, \ \ \forall i \in [1, \ldots, N] \end{cases} \tag{12}$$

The problem admits solution if $\sum_{i=1}^{N} C^{(i)}_{\min} < C$; otherwise

the allocation is performed as

$$C^{(i)} = \left(C / \sum_{i=1}^{N} C_{\min}^{(i)} \right) C_{\min}^{(i)} \tag{13}$$

In other words, if the bandwidth is not sufficient to guarantee the QoS requirements, it is allocated proportionally to the minimum capacity required.

3.2. The cost function in the CAP case

A strong penalization is introduced if the average call blocking probability of the system is above the fixed threshold. The penalty function introduced is:

$$F_{\mathrm{CAP}}^{(i)}(Z^{(i)}) = \begin{cases} 0 & \text{if } \bar{P}_B^{(i)}\left(N_{\max}^{(i)}(Z^{(i)})\right) \le \gamma^{(i)} \\ H & \text{if } \bar{P}_B^{(i)}\left(N_{\max}^{(i)}(Z^{(i)})\right) > \gamma^{(i)} \end{cases} \tag{14}$$

The function $\bar{P}_B^{(i)}(\cdot)$ is defined as the call blocking probability of station i, averaged over the fading levels.

$$\bar{P}_B^{(i)}\left(N_{\max}^{(i)}(Z^{(i)})\right) = \sum_{\mathrm{level}=1}^{F} p_{\mathrm{level}}^{(i)} P_B^{(i)}\left(N_{\max}^{(i)}(Z^{(i)})\right) \tag{15}$$

$P_B^{(i)}(\cdot)$ has been defined in Eq. (1), and F is the number of fade degradation levels.

The cost function of station i is:

$$J_{\mathrm{CAP}}^{(i)}(Z^{(i)}) = \bar{P}_{\mathrm{loss}}^{(i)}\left[C_{\mathrm{ng}}^{(i)}(Z^{(i)}), N_{\max}^{(i)}(Z^{(i)}) \right] + F_{\mathrm{CAP}}^{(i)}(Z^{(i)}) \tag{16}$$

The global cost to be minimized is now:

$$J_{\mathrm{CAP}}(Z^{(1)}, Z^{(2)}, \ldots, Z^{(N)}) = \sum_{i=1}^{N} \sum_{\mathrm{level}} p_{\mathrm{level}}^{(i)} J_{\mathrm{CAP}}^{(i)}\left(\beta_{\mathrm{level}}^{(i)} Z^{(i)}\right) \tag{17}$$

4. The control scheme in the remote stations

The lower level allocation algorithm acts with a faster timing than the upper one, and it is located in each remote earth station i. It shares the bandwidth $C^{(i)}$, allocated to station i, between guaranteed ($C_{\mathrm{g}}^{(i)}$) and non-guaranteed ($C_{\mathrm{ng}}^{(i)}$) traffic, by imposing a constraint on the call blocking probability. It performs call admission control of the incoming guaranteed calls and measures the statistics necessary for successive allocations.

Given the bandwidth $C^{(i)}$, allocated to station i, the lower level optimization problem evaluates the threshold $N_{\max}^{(i)}$ such that the call blocking probability (1) be, if possible, lower than $\gamma^{(i)}$. $N_{\max}^{(i)}$ may assume values in the range $[0, \ldots, \lfloor C^{(i)}/B \rfloor]$.

Having computed (off-line) the minimum bandwidth $C_{\min}^{(i)}$ that satisfies the constraint,

$$C_{\min}^{(i)} = \arg\min_{X^{(i)}} \left\{ X^{(i)} \in \mathscr{R} : P_B^{(i)}(\lfloor X^{(i)}/B \rfloor) \le \gamma^{(i)} \right\} \tag{18}$$

the minimum threshold will be

$$N_{\max}^{(i)} = \begin{cases} \left\lfloor C_{\min}^{(i)}/B \right\rfloor & \text{if } C_{\min}^{(i)} < C^{(i)} \\ \lfloor C^{(i)}/B \rfloor & \text{if } C_{\min}^{(i)} \ge C^{(i)} \end{cases} \tag{19}$$

If the bandwidth allocated by the upper layer is higher than the minimum threshold, the available bandwidth is shared between the guaranteed and non-guaranteed flow, assuring a portion sufficient to provide the required QoS (represented by $\gamma^{(i)}$) for synchronous traffic. If the value of $C^{(i)}$ is lower than the minimum bandwidth required, all the bandwidth is given to synchronous traffic.

Both from the computational and the technological point of view, it is simpler to assume:

$$C^{(i)} \in \mathscr{R} : C^{(i)} = k \text{ mbp},\ k \in N,\ C^{(i)} \le C$$

If the minimum portion of bandwidth is very small, the algorithm is very flexible, but the computational load increases.

5. A case study based on real attenuation values

Let us see now how the model of the faded channel, we assumed in the previous CAP case, maps into reality. In particular, we want to estimate the probability that the coefficient $\beta_{\mathrm{level}}^{(i)}$, which depends on the channel degradation, assumes certain values. We compare the CAP and the OC bandwidth allocation schemes numerically, by using fade probabilities' estimates from real weather attenuation experimental data. The parameters relevant to the satellite network are computed considering a bent-pipe geostationary satellite (i.e. the satellite is only a repeater and it does not perform any demodulation of data). In particular, the link budget values are relevant to the transponder #1 of the Italsat national coverage payload, which operates in the 20–30 GHz band [13]. The master station operates with a larger antenna than the slave stations' one. We only consider the in-bound link that supports the traffic directed from the slaves to the master, which is attached to one or more LANs and it is seen as the major traffic concentrator.

The in-bound link is shared in TDMA mode among the traffic stations, while the out-bound link, from the master to slaves, operates in TDM. Communications between slaves undergo a double satellite hop through the master. In order to compute the probability of $\beta_{\mathrm{level}}^{(i)}$, the fade on the up-link only is considered, because the link budget is of up-link predominant type. Thus, the power margin of 7.5 dB, assumed in the down-link, allows us to decouple the up/down-link fades. In Table 1, the most significant parameters of the system are reported.

The total system information rate of 8.192 Mbits/s is obtained with a 4/5 punctured convolutional coder/Viterbi decoder [2] at 7 dB of E_b/N_0 (bit energy to one-sided noise spectral density ratio), which is the reference value in clear

Table 1
Most significant values of the TDMA system considering the Italsat satellite

Master station's antenna diameter	3 m
Slave stations' antenna diameter	1.2 m
Slave stations' power	13 dB W
Satellite *G/T*	5.9 dB/K
Satellite *EIRP* (effective isotropic radiation power)	48 dB W
Carrier capacity	10.24 Mbit/s
Power margin in clear sky conditions	2 dB
Ref. net E_b/N_0 (clear sky conditions)	7 dB
Bit error rate guaranteed	10^{-7}
Possible data coding rates	4/5 (clear sky), 2/3, 1/2
Information bit rate in clear sky conditions	8.192 Mbit/s

sky conditions, keeping into account 1 dB of modem implementation margin.

In order to compute the probabilities of $\beta_{\text{level}}^{(i)}$, we refer to the ITU-R interpolation formula [14]:

$$A_p = A_{0.01} 0.12 p^{-(0.546+0.043 \log p)} \tag{20}$$

which estimates the attenuation exceeded for a percentage p of an average year, when the attenuation $A_{0.01}$ exceeded for 0.01% of a year is known for a given site. In Table 2, the attenuation parameters are reported for two different classes of stations, which we denote as type 1 and type 2. Relation (20) is plotted in Fig. 1.

The $A_{0.01}$ values, taken from Ref. [15], are the frequency scaled attenuation values resulting from 5 years of Sirio experiments at Fucino (type 1 stations) and Lario (type 2 stations), two Italian sites with very different climatic characteristics, in the center and in the north of Italy, respectively.

Table 3 contains the probability that the fade level of the slave stations falls into certain intervals, called *fade classes*. Each fade class imposes the adoption of the indicated trans-

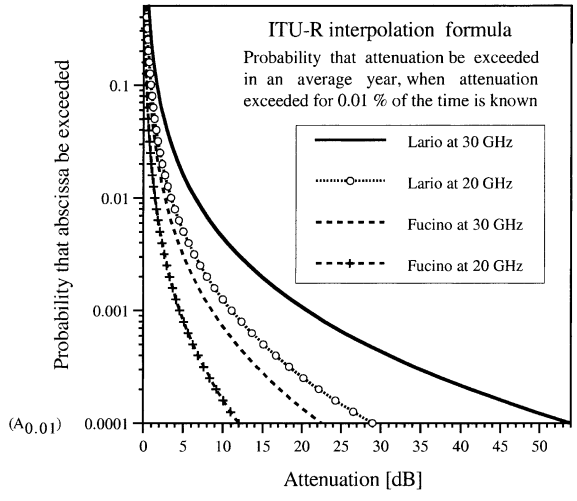

Fig. 1. The ITU-R interpolation formula graph for Lario and Fucino stations at 20–30 GHz.

Table 2
Attenuation-dependent parameters for two different classes of stations

Station type	$A_{0.01}$ (dB) (up-link)	$A_{0.01}$ (dB) (down-link)	Master station down-link availability (%) (7.5 dB power margin)
Type 1	22.5	12	99.97
Type 2	52.3	28.4	99.78

mission parameters (and then $\beta_{\text{level}}^{(i)}$ values) to limit the bit error rate below the chosen threshold of 10^{-7}.

6. OC and CAP comparison in the case study

We evaluate the effect of the knowledge of the a-priori probabilities of the fading levels by comparing the OC and CAP strategies in the case of four stations, first, in a very unbalanced situation, deriving from a partial observation of local meteorological conditions. Three stations (namely, numbers 1, 2, and 3) are known to operate in clear sky, whereas one (station 4) is affected by rain, whose intensity, however, is not precisely known to the master. Successively, we extend the analysis to all possible cases to get an overall evaluation of the systems' behaviors. If $\beta^{(i)}$ indicates the random variable that assumes values $\beta_{\text{level}}^{(i)}$, we thus have $\beta^{(i)} = 1$, $i = 1, 2, 3$ with probability 1, $\beta^{(4)} = 1$ with probability 0, and we should substitute the probabilities of the other values of $\beta^{(4)}$ with the corresponding conditional probabilities $\Pr\{\beta^{(4)} = \beta_{\text{level}}^{(4)} | \text{rain}\}$. The latter are easily obtained as:

$$\Pr\left\{\beta^{(4)} = \beta_{\text{level}}^{(4)} | \text{rain}\right\} = \frac{\Pr\left\{\beta^{(4)} = \beta_{\text{level}}^{(4)}\right\}}{(1 - \Pr\{\text{clear sky}\})}$$

Another probability, conditioned to rain, but not in outage conditions, given by:

$$\Pr\left\{\beta^{(4)} = \beta_{\text{level}}^{(4)} | \text{rain} | \text{not in outage}\right\}$$

$$= \Pr\left\{\beta^{(4)} = \beta_{\text{level}}^{(4)} | \text{rain}\right\} / (1 - \Pr\{\text{outage}\})$$

is used to evaluate the cost function (17). This has been done for two reasons. The first one is to impose no constraints to the choice of $\gamma^{(i)}$, which otherwise would be lower-bounded by the outage probability conditioned to a rain event. The other reason is to limit the unbalance of the bandwidth allocation in favor of the faded stations. After that the allocation pattern is computed, the performance indexes are obviously evaluated without any no-outage conditioning of $\beta^{(i)}$.

Let us assume station 4 to be of type 2 (Lario type). Values are reported in Table 4. Note that the probabilities referred in the following are all conditioned to the fact that station 4 is in rain conditions and stations 1, 2, and 3 are in clear sky.

The calculations have been performed in a number of test

Table 3
Relationships between slave station up-link fade classes, probability and $\beta_{\text{level}}^{(i)}$, for two different station classes. C_d denotes the coding rate and B_r denotes the bit rate

Fade level (dB)	$\beta_{\text{level}}^{(i)}$ Prob. (%) (type 1 stat.)	$\beta_{\text{level}}^{(i)}$ Prob. (%) (type 2 stat.)	$\beta_{\text{level}}^{(i)}$	C_d, B_r (Mbit/s)	Net E_b/N_0 (dB)
0 ÷ 2	98.29	92.90	1	4/5, 10.24	7
2 ÷ 5	1.39	5.54	1/1.2	2/3, 10.24	4.5
5 ÷ 7	0.17	0.76	1/1.6	1/2, 10.24	2.5
7 ÷ 10	0.08	0.39	1/3.2	1/2, 5.12	2.5
10 ÷ 13	0.03	0.16	1/6.4	1/2, 2.56	2.5
> 13	0.04	0.25	–	Outage	–

Table 4
Conditional probabilities in the event of rain observed at station 4

$\beta_{\text{level}}^{(4)}$	$Pr\{\beta^{(4)} = \beta_{\text{level}}^{(4)}\|\text{rain}\}$	$Pr\{\beta^{(4)} = \beta_{\text{level}}^{(4)}\|\text{rain}\|\text{not in outage}\}$
1	0	0
0.83333	0.7805	0.8080
0.625	0.1076	0.1114
0.3125	0.0547	0.0566
0.15625	0.0231	0.0240
0	0.0341	0

cases, obtained by linearly increasing both synchronous and asynchronous loads, according to Table 5. The value of $\gamma^{(i)}$ has been chosen equal to 5% for all stations.

The synchronous traffic load is expressed in Erlangs. For all tests presented, the average duration of the connections is $1/\mu^{(1)} = 180$ s, $\forall i$, the connections' capacity is 16 kbit/s, and the minimum bandwidth portion (mbp) that can be allocated is 8 kbit/s.

Fig. 2 shows the behavior of the blocking probability for the synchronous traffic at the various loads in the two control situations. They are equal (as desirable) for stations operating in 'clear sky', whereas there is some advantage in the CAP case for the station in fading conditions (more bandwidth is allocated, resulting in the possibility to keep blocking below the threshold at higher load).

Table 5
Load distribution for the test cases

Test #	Station 1		Station 2		Station 3		Station 4	
	$\rho^{(1)}$	$\lambda_{\text{burst}}{}^{(1)}$	$\rho^{(2)}$	$\lambda_{\text{burst}}{}^{(2)}$	$\rho^{(3)}$	$\lambda_{\text{burst}}{}^{(3)}$	$\rho^{(4)}$	$\lambda_{\text{burst}}{}^{(4)}$
1	20	100	20	100	10	50	10	50
2	22	120	22	120	11	60	11	60
3	24	140	24	140	12	70	12	70
4	26	160	26	160	13	80	13	80
5	28	180	28	180	14	90	14	90
6	30	200	30	200	15	100	15	100
7	32	220	32	220	16	120	16	110
8	34	240	34	240	17	140	17	120
9	36	260	36	260	18	160	18	130
10	38	280	38	280	19	180	19	140
11	40	300	40	300	20	200	20	150

It is worth noting that at station 4 the threshold $\gamma^{(4)} = 5\%$ is exceeded. This is the effect produced by assuming the probability conditioned to rain, but not in outage conditions, to evaluate the cost function. The target value considered by the system is then $\gamma^{(4)} + P\{\text{outage}|\text{rain}\}$. The last term in this case is 3.4% (see Table 4). CAP allows to remain below the threshold in all tests, whereas OC does not in some cases. The behavior of stations 3 and 4 (a sudden decrease in the blocking probability) is caused by a unity increase in the maximum number of connections allowed $N_{\max}^{(i)}$, which becomes necessary to stay below the threshold.

As regards the upper bound of the overflow probabilities, we show the behavior at stations 1, 2, and 3 in Fig. 3 (stations 1 and 2 present the same performance), while Fig. 4 depicts the situation of station 4.

It can be noted that the two strategies have an opposite behavior. In particular, the information on the fading levels and their likelihood, exploited by CAP, allows the latter to protect station 4 effectively, at the expense of a slight degradation in the same performance index at the other stations.

In order to make a more exhaustive investigation on the performance of the two algorithms, we extend the above analysis to all possible cases, and then we merge all cases together to get the cumulative distribution function (CDF) that given values of overflow and blocking are not exceeded. In order to have fewer parameters to change to show the

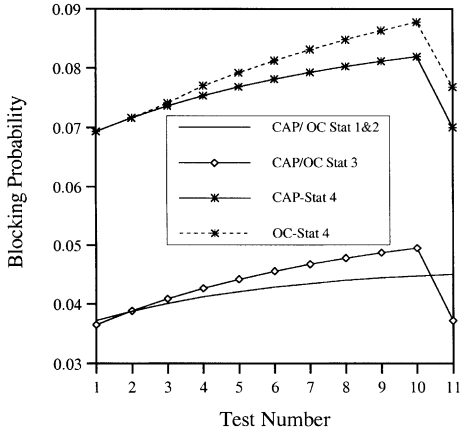

Fig. 2. Blocking probabilities at stations 1, 2, 3, and 4.

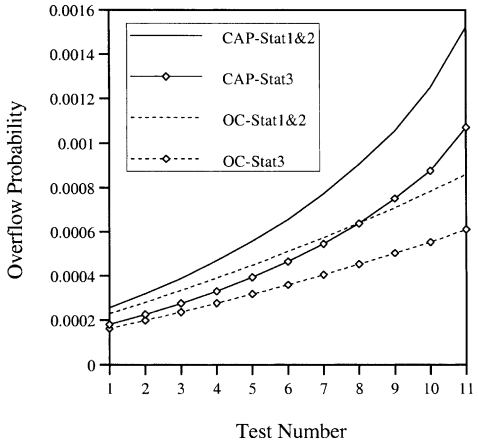

Fig. 3. Overflow probability at stations 1, 2, and 3.

performance scenario, we suppose to have all stations with the same climatic characteristics and equally loaded.

We then show the performance indexes of one station, say station 1, which also represent the average indexes of the whole network. From station 1's standpoint, the number of possible cases is two times the number of stations. In fact, station 1 can be in rain conditions or not, and for both cases i stations ($i = 0, \ldots, N-1$) can be in rain conditions.

In order to evaluate the probabilities of all possible cases, we refer to Refs. [1,15], where the data of the Sirio experiment were employed to estimate the joint attenuation distributions using three stations: Lario, Spino d'Adda, and Fucino. In a region that excludes very low and large attenuation levels, Refs. [1,15] show that the measured joint distributions of each pair of stations differ approximately by a multiplicative factor k from the joint distributions that would have been obtained from the marginal distributions in the case of statistical independence. For the tested frequency (11.6 GHz), the factor k was found to be equal to 20 for the Lario–Spino (85 km) pair, and equal to 4 and 2 for Spino–Fucino (510 km) and Lario–Fucino (570 km), respectively. Let us now extend these results to a higher number of stations operating at 30 GHz, and consider cases in which the attenuation probability curves and the parameters k are the same for all stations. This last hypothesis is not realistic, because it is practically impossible that many stations all have the same dependence on each other. However, we need to express system performance as a function of a single parameter, which should then be considered as an average value, or a maximum experimental value, if a conservative result is preferred. Recalling that N is the number of stations, denote by p_f the unconditional probability that each station be in fade (p_f is the same for all stations), by $p_{nf}^{(i)}$ the probability that station 1 is not faded and i stations are faded, by $p_f^{(i)}$ the probability that station 1 is faded and i of the other stations are faded. The probabilities of all $2N$ cases are

$$p_{nf}^{(i)} = \binom{N-1}{i}(1-kp_f)^{N-i}p_f^i k^{i-1}, \qquad i = 1, \ldots, N-1 \tag{21}$$

$$p_{nf}^{(i)} = 1 - \sum_{j=1}^{N}\binom{N-1}{j}k^{j-1}p_f^j(1-kp_f)^{N-j}, \qquad i = 0$$

$$p_f^{(i)} = \binom{N-1}{i}(1-kp_f)^{N-i-1}p_f^{i+1}k^i, \qquad i = 0, \ldots, N-1$$

The cases with probability $p_{nf}^{(i)}$ have a unitary probability that $\beta_{level}^{(1)} = 1$, while the $p_f^{(i)}$ cases have the probability of $\beta_{level}^{(1)}$ given by the first two columns of Table 4. The number of all non-null cases, which contribute to build the CDF of the system parameters, is then $6N$, including the outage cases. In Figs. 5–8, a scenario is reported, which shows the CDFs of the overflow and the blocking probabilities for both CAP and OC algorithms and for different values of some system's parameters. All figures report the values of two probabilities on both axes. This may look like non-sense at a first glance. However, we must consider that we are dealing with parameters averaged over a year time interval and, therefore, even very small fractions of time, like the ones involved in our computations, are long enough to build statistics.

The differences between CAP and OC systems, evidenced in the above figures, may not appear relevant. However, the following considerations, made from the system acceptability point of view, will help us to evaluate the differences. Let us consider the situation depicted in Fig. 5(a). If we choose a 1% threshold of the overflow probability to declare the system acceptable, we see that CAP guarantees not to exceed this threshold for a 99.75% of time in a year, while OC reaches only 99.6%. This is translated into 22 h of non-acceptability, which practically coincides with the outage period, in the CAP case, versus the 36 h in the OC case. Considering the attenuation probability curve of Fig. 1 (case of up-link Lario type stations) we can translate the above acceptability conditions into the fact that CAP can

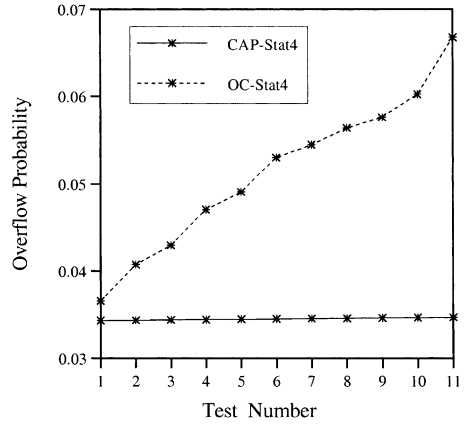

Fig. 4. Overflow probability at station 4.

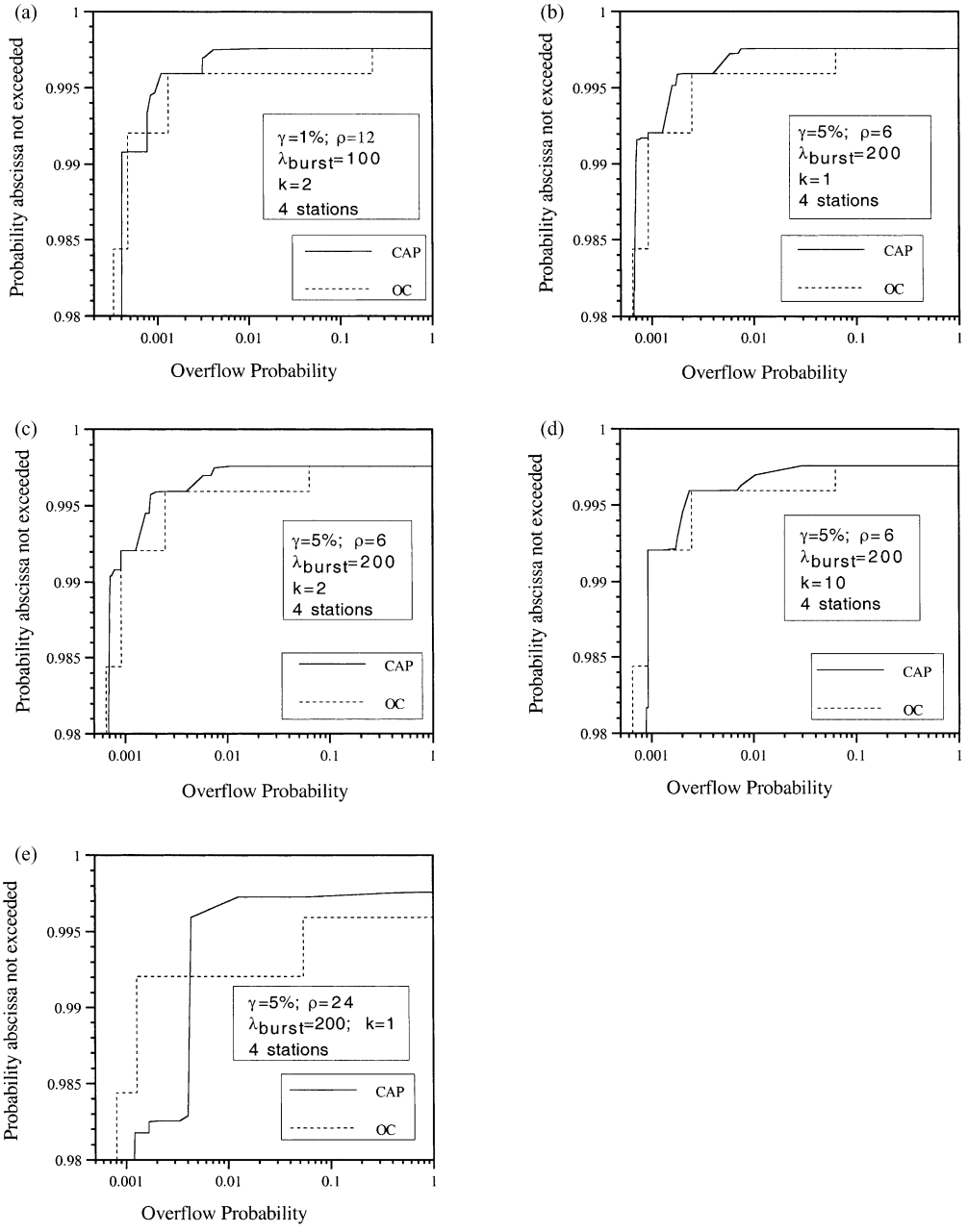

Fig. 5. Cumulative probability of overflow for different parameter values.

support 2.8 dB of attenuation more than OC. We can also say that CAP can reach the same performance (1% overflow probability threshold) as OC, operating with a power 2.8 dB lower than OC.

In Table 6, we report the non-availability time and the maximum attenuation supported by both systems, together with the total overflow and blocking probabilities, averaged over an entire year, for the parameter configurations used in the figures. The values reported in the last five columns of Table 6 generally vary with the threshold chosen. We can see that the advantage of CAP over OC grows with the number of stations, while it decreases with a higher dependence of the stations' meteorological conditions (higher k factor), as expected.

7. Conclusions

The effect of the knowledge of 'a-priori' probabilities of fading levels (derived from long-term statistical measures) on the bandwidth allocation among different earth stations and traffic classes in a satellite channel has been investigated in the paper. In particular, we have defined a control strategy that exploits the above information, and compared its

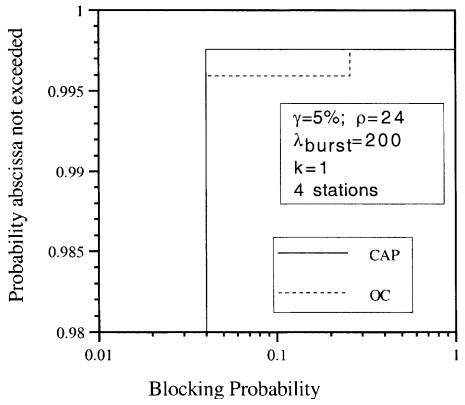

Fig. 6. Cumulative blocking probability.

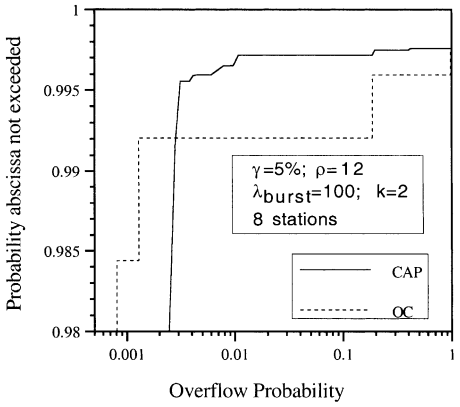

Fig. 7. Cumulative probability of overflow (eight stations).

performance with one that does not. The macroscopic effect of fading has been modeled essentially as a reduction in the effective bandwidth seen by a station. In order to enhance the different situations, a simple real-time observation ('rain'—clear sky) has been introduced, which, however, does not distinguish among the possible fade depths; the latter are still characterized by their 'a priori' probabilities. The overall performance in terms of availability and robustness to attenuation level has been evaluated in a case study, by considering all possible weather scenarios (along with the corresponding fading levels) and their empirical probabilities, derived from long-term observations. We have shown by numerical comparisons that, even though this model does not address short-term fading behavior (which would require real-time observations of the 'instantaneous' fade levels), yet it allows some gain over a completely 'blind' situation. The combination of long-term assignments as the ones considered here with dynamic assignments, coping with short-term variations, is a matter of current investigation.

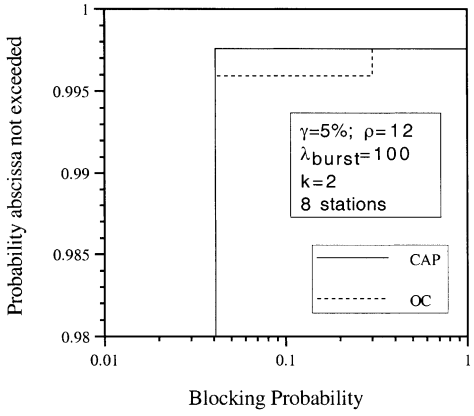

Fig. 8. Cumulative blocking probability (eight stations).

Table 6
Some system characteristics

System parameters	Overflow total probability (%) (averaged over 1 year)		Total blocking probability (%) (average over 1 year)		System unavailability (hours/year) (1% overflow prob. threshold)		Attenuation supported (dB) (1% overflow prob. threshold)		
	CAP	OC	CAP	OC	CAP	OC	CAP	OC	Δ
4 stat., $k = 2$, $\gamma = 1\%$, $\rho = 12$, $\lambda_{burst} = 100$	0.27	0.30	1.2	1.2	22	36	12.9	10.1	2.8
4 stat., $k = 1$, $\gamma = 5\%$, $\rho = 6$, $\lambda_{burst} = 200$	0.30	0.30	4.54	4.54	21	38	13.1	9.8	3.3
4 stat., $k = 10$, $\gamma = 5\%$, $\rho = 6$, $\lambda_{burst} = 200$	0.30	0.30	4.54	4.54	26	38	11.7	9.7	2.0
4 stat., $k = 1$, $\gamma = 5\%$, $\rho = 24$, $\lambda_{burst} = 200$	0.33	0.49	4.24	4.28	36	70	10.1	7.1	3.0
8 stat., $k = 2$, $\gamma = 5\%$, $\rho = 12$, $\lambda_{burst} = 100$	0.33	0.54	4.32	4.36	31	70	10.9	7.1	3.8

Acknowledgements

This work was partially supported by the Italian National Research Council (C.N.R.), under the '5%' Multimedia Program. The authors wish to thank Dr Eng. Claudio Balestrino for his precious support in the numerical calculation programs.

References

[1] F. Carassa, Adaptive methods to counteract rain attenuation effects in the 20/30 GHz band, Space Commun. Broadcasting 2 (1984) 253–269.
[2] N. Celandroni, E. Ferro, N. James, F. Potortì, FODA/IBEA: a flexible fade countermeasure system in user oriented networks, Internat. J. Satellite Commun. 10 (6) (1992) 309–323.
[3] B. Tsybakov, N.D. Georganas, On self-similar traffic in ATM queues: definition, overflow probability bound, and cell delay distribution, IEEE/ACM Trans. Networking 5 (3) (1997) 397–409.
[4] R. Bolla, F. Davoli, Control of multirate synchronous streams in hybrid TDM access networks, IEEE/ACM Trans. Networking 5 (2) (1997) 291–304.
[5] F. Davoli, P. Maryni, A two-level stochastic approximation for admission control and bandwidth allocation, IEEE J. Selected Areas Commun. 18 (2) (2000) 222–233 Special issue on intelligent techniques in high-speed networks.
[6] K.W. Ross, D.H.K. Tsang, Optimal circuit access policies in an ISDN environment: a Markov decision approach, IEEE Trans. Commun. COM-37 (1989) 934–939.
[7] G. Meempat, M. Sundareshan, Optimal channel allocation policies for access control of circuit-switched traffic in ISDN environments, IEEE Trans. Commun. 41 (1993) 338–350.
[8] J.E. Wieselthier, A. Ephremides, Fixed- and movable-boundary channel-access schemes for integrated voice/data wireless networks, IEEE Trans. Commun. 43 (1) (1995) 64–74.
[9] K. Gokbayrak, C.G. Cassandras, Adaptive call admission control in circuit-switched networks, IEEE Trans. Automat. Contr. (2002) Special issue on systems and control methods in communication networks.
[10] B. Tsybakov, N.D. Georganas, Overflow probability in ATM queue with self-similar input traffic, Proceedings of the IEEE International Conference on Communication (ICC'97), Montreal, Canada, 1997.
[11] S. Ghani, M. Schwartz, A decomposition approximation for the analysis of voice/data integration, IEEE Trans. Commun. 42 (1994) 2441–2452.
[12] R. Bolla, F. Davoli, M. Marchese, A bandwidth allocation strategy for multimedia traffic in a satellite network, Proceedings of the IEEE Globecom2000, San Francisco, CA, 2000, pp. 1130–1134.
[13] F. Carducci, M. Francesi, The Italsat satellite system, Internat. J. Satellite Commun. 13 (1995) 49–81.
[14] ITU-T Report 564-4, Propagation Data and Prediction Methods Required for Earth-Space Telecommunication Systems, 1990.
[15] F. Carassa, E. Matricciani, G. Tartara, Frequency diversity and its application, Internat. J. Satellite Commun. 6 (3) (1988) 313–322.